Carbohydrate Polymers 133 (2015) 473–481

Contents lists available at ScienceDirect

Carbohydrate Polymers

journal homepage: www.elsevier.com/locate/carbpol

# Bifunctionalized dextrans for surface PEGylation via multivalent host–guest interactions

Iurii Antoniuk[a], Véronique Wintgens[a], Gisèle Volet[a], Thorbjørn T. Nielsen[b], Catherine Amiel[a,*]

[a] University Paris Est, ICMPE (UMR 7182), CNRS, UPEC, F-94320 Thiais, France
[b] Department of Chemistry and Bioscience, Aalborg University, Fredrik Bajers Vej 7H, 9220 Aalborg Ø, Denmark

ARTICLE INFO

*Article history:*
Received 29 April 2015
Received in revised form 15 June 2015
Accepted 8 July 2015
Available online 22 July 2015

*Keywords:*
Modified dextrans
Cyclodextrin polymers
Supramolecular association
Surface films
PEGylation

ABSTRACT

The main goal of this work was to develop a supramolecular chemistry strategy to decorate interfaces with polyethylene glycol (PEG) grafts. A series of novel bifunctionalized dextrans, bearing 40–60 PEG pending chains and 12–24 hydrophobic adamantyl groups, have been prepared by copper(I)-catalyzed azide-alkyne cycloaddition. Their binding properties toward native βCD and βCD polymers were characterized both in solution and at interface using isothermal titration microcalorimetry and surface plasmon resonance. The polymers were found to form stable layers onto neutral and positively charged βCD-polymer films pre-adsorbed on gold surfaces, due to multivalent interpolymer host–guest interactions. The thickness and stability of the layers could be tuned by varying the ratio between the degrees of substitution by PEG and adamantyl groups.



## 1. Introduction

Two key requirements for polymeric nanocarriers to be successfully applied in controlled delivery and release are high sterical stability and robust protection from the uptake by the blood mononuclear phagocyte system (MPS) (Gaucher, Dufresne, Sant, Maysinger, & Leroux, 2005; Li & Huang, 2008; Vonarbourg, Passirani, Saulnier, & Benoit, 2006). One of the preferred and well-established ways to meet these consists in decorating the surface of nanoparticles with polyethylene glycol (PEG), often referred as PEGylation (Gaucher et al., 2005). The presence of hydrophilic and highly flexible PEG chains in contact with physiological media proved to significantly reduce the opsonin proteins adsorption, thereby increasing the average blood circulation times of nanocarriers (Immordino, Dosio, & Cattel, 2006; Jokerst, Lobovkina, Zare, & Gambhir, 2011; Loira-Pastoriza, Todoroff, & Vanbever, 2014). Besides providing steric stabilization and stealth properties, PEG "corona" usually leads to higher apparent sizes, thus increasing the efficiency of a nanocarrier administration due to the enhanced permeability and retention effect (EPR). The PEGylation might be achieved in various ways, including preparation of PEG-containing block copolymers for polymeric micelles formation (Gaucher et al., 2005), covalent modification (Roberts, Bentley, & Harris, 2002; Yoncheva, Lizarraga, & Irache, 2005) or physical adsorption by "host–guest" interactions (David, Millot, Sebille, & Levy, 2003; Pun & Davis, 2002; Volet & Amiel, 2012).

Cyclodextrins (CD) are cyclic (α-1,4)-linked oligosaccharides consisting of six, seven or eight α-D-glucopyranose in the case of the most common α-, β- and γ-cyclodextrins respectively. They are characterized by toroidal shape with hydrophilic exterior and hydrophobic internal cavity, which allows them to form inclusion complexes with various hydrophobic substrates (Loftsson & Brewster, 1996). This property has led to the widespread use of cyclodextrin-based materials in biomedical and personal care industry as excipients, drug carriers and solubility enhancers (Brewster & Loftsson, 2007; Hedges, 1998; van de Manakker, Vermonden, van Nostrum, & Hennink, 2009). During the last two decades a high number of researches were aiming at diminishing the phenomenon of initial "burst release" of actives from nanoscale drug delivery carriers (Wu & Brazel, 2008). Along with superficial cross-linking, adsorption or impregnation of drug carriers with CD-containing materials was found to be an efficient strategy to address this issue. For instance, it was reported that co-encapsulation of hydroxypropyl-βCD into poly(lactide-co-glycolide) (PLGA) microspheres led to a significant decrease of the initial "burst" of loaded insulin (Quaglia et al., 2003); benzophenone-loaded

* Corresponding author.
*E-mail addresses:* antoniuk@icmpe.cnrs.fr (I. Antoniuk), wintgens@icmpe.cnrs.fr (V. Wintgens), volet@icmpe.cnrs.fr (G. Volet), ttn@bio.aau.dk (T.T. Nielsen), amiel@icmpe.cnrs.fr (C. Amiel).

http://dx.doi.org/10.1016/j.carbpol.2015.07.027
0144-8617/

polylactic acid (PLA) nanoparticles were covered with neutral poly-βCD and shown to have improved kinetic profile of the benzophenone release, governed by its "host–guest" interactions with βCDs in the shell (El Fagui & Amiel, 2012). In a more recent example membrane fusion between liposomes and cyclodextrin vesicles was used to prepare hybrid assemblies comprised of liposomal core covered with layers of βCD amphiphiles (Versluis et al., 2014). Another way for introducing βCD in nanoscale drug carriers consists in assembling βCD polymers with "guest"-labeled amphiphilic copolymers (Ren, Chen, & Jiang, 2009; Wintgens, Nielsen, Larsen, & Amiel, 2011).

In this work we present a possible path for combination of the benefits of PEGylation and βCD-containing materials. Although several works have already reported the host–guest anchoring of PEG chains onto β-cyclodextrin containing surfaces (David et al., 2003), to the best of our knowledge, only few studies of the multivalence effect, when multiple PEPO (Pluronics) grafts and guest groups are attached to a polymer backbone, have been done so far (Wintgens, Layre, Hourdet, & Amiel, 2012). We report a synthesis of novel (PEG, Ada)-grafted dextrans, prepared by copper-catalyzed azide-alkyne cycloaddition (CuAAC). These bifunctionalized "guest" polymers are bearing various amounts of 5000 g/mol PEG chains and hydrophobic adamantyl (Ada) groups at the same time. The ability of (PEG, Ada)-grafted dextrans to form inclusion complexes in solution and on surface with native βCD and βCD polymers are investigated with the purpose of their further use for facile PEGylation of interfaces and nanoparticles via multivalent host–guest interactions.

## 2. Materials and methods

### 2.1. Materials

Pyridine (99.9%, anhydrous), *N*,*N*′-dimethylformamide (DMF, 99.8%, anhydrous), tetrakis(acetonitrile)copper(I)tetrafluoroborate ($Cu(MeCN)_4PF_6$, 97%), thionyl chloride ($SOCl_2$, 99+%), 1-adamantaneethanol (98%) and glycidyl propargyl ether (GPE, 90+%) were purchased from Sigma–Aldrich (Saint Quentin Fallavier, France) and used as received. p-Toluenesulfonyl chloride (98%), sodium azide (99%), L-ascorbic acid sodium salt (Na-Asc, 99%) and dimethyl sulfoxide (DMSO, 99.8%, anhydrous) were purchased from Alfa Aesar and used as received. Sodium hydroxide (98+%, anhydrous pellets) were purchased from Acros Organics and used as received.

Dextran (DT40, $M_w = 4.3 \cdot 10^4$ g/mol, PDI = 1.5, Amersham Pharmacia Sweden), lithium chloride (Alfa Aesar) and poly(ethylene glycol) methyl ether of 5000 Da (MeOPEG-OH, Sigma–Aldrich) were dried overnight in vacuum at 90 °C prior to use.

Tris[(1-benzyl-1H-1,2,3-triazol-4-yl)methyl]amine (TBTA) (Chan, Hilgraf, Sharpless, & Fokin, 2004) was synthesized according to the literature data. Neutral epichlorohydrin-branched pβCD polymer and positively charged pβCDN+, modified with quaternary ammonia, were prepared according to the previously described procedures (Blomberg, Kumpulainen, David, & Amiel, 2004; Renard, Deratani, Volet, & Sebille, 1997).

### 2.2. Synthesis

The syntheses under microwave irradiation (MW) were performed using a Monowave-300 reactor from Anton Paar. The microwave source was a magnetron with a 2.5 GHz frequency powered by a 900 W power generator, which could be operated at different power levels. The reaction mixtures were loaded inside quartz glass tubes; the tubes were closed with silicon caps using a pressure monitor unit, and placed into the reactor. The microwave reactor was programmed to maintain a constant temperature by adjusting the applied power; the desired temperature was reached gradually using an initial 3 min temperature ramp. After the end of the reaction, solutions were cooled to room temperature with compressed air. When necessary, ultrafiltration was carried out under $N_2$ atmosphere using Amicon equipment and regenerated cellulose membranes with MWCO 30,000. Dialysis was done with Spectra/Por molecular porous tubing MWCO 6000–8000. The ultrafiltrated and dialyzed solutions were freeze-dried on CHRIST ALPHA 1–2 LD Plus lyophilizator.

Short names of the polymers were attributed using the following pattern: D40-*X*GP-*Y*Ada-*Z*PEG with *X*, *Y* and *Z* indicating the molar degree of substitution (DS) of anhydroglucosidic rings (further AHG) by different substituents.

#### 2.2.1. Ada-$N_3$

*2.2.1.1. 1-Adamantaneethyltosylate.* 1-Adamantaneethanol (4.80 g, 26.6 mmol) was dissolved in 25 mL of pyridine, cooled to 0 °C on ice bath and p-toluenesulfonyl chloride (8.37 g, 43.9 mmol) was added to the solution. The reaction mixture was allowed to warm and stirred overnight at room temperature. The solvent was evaporated under reduced pressure and the product was redissolved in 100 mL of EtOAc. The organic layer was washed once with saturated $NaHCO_3$ and twice with brine, dried over $Na_2SO_4$, filtered and evaporated under reduced pressure. The subsequent filtration through a silica pad (40 g, EtOAc/n-heptane = 1/25) yielded the final product as a white solid. Thin layer chromatography (TLC) was carried out using Silica gel 60 $F_{254}$ TLC plates with 0.2 mm silica gel (EtOAc/heptane = 1/25). Yield: 89.4% (7.96 g). $^1$H NMR (DMSO-$d_6$) $\delta$ = 1.30–1.40 (m, 6H + 2H, Ada overlapped with Ada-C$H_2$), 1.45–1.70 (m, 6H, Ada), 1.90 (s, 3H, Ada), 2.42 (s, 3H, —$CH_3$), 4.03 (t, 2H, C$H_2$-OTs), 7.49 (d, 2H, Ts), 7.78 (d, 2H, Ts).

*2.2.1.2. 1-Adamantaneethylazide (Ada-$N_3$).* 1-Adamantaneethyltosylate (7.96 g, 23.8 mmol) was dissolved in 0.5 mol/L $NaN_3$ solution in DMSO (167 mL, 83.3 mmol) and stirred at 80 °C for 50 h. 250 mL of water were added to quench the reaction, and after cooling down 800 mL of EtOAc were added. The organic phase was washed 3 times with water and one time with brine, dried over $Na_2SO_4$ and filtered. Concentration under reduced pressure and drying under vacuum gave yellowish oil. Yield: 74.6% (3.64 g). The IR spectrum of the product showed a single —$N_3$ peak at 2094 $cm^{-1}$. $^1$H NMR ($CDCl_3$) $\delta$ = 1.38 (t, 2H, Ada-C$H_2$), 1.48 (s, 6H, Ada), 1.57–1.72 (m, 6H, Ada), 1.94 (s, 3H, Ada), 3.24 (t, 2H, C$H_2N_3$).

#### 2.2.2. MeOPEG-$N_3$

*2.2.2.1. MeOPEG-Cl.* MeOPEG-OH (10 g, 2 mmol) of 5000 g/mol was dissolved in 15 mL (206.5 mmol) of $SOCl_2$; the reaction mixture was heated to 85 °C and refluxed for 40 h. Excess $SOCl_2$ was removed by bubbling argon at 65 °C. Then 100 mL of DCM were added and the obtained solution was precipitated in 1 L of $Et_2O$, filtered and washed with $Et_2O$. The subsequent drying in vacuum at 40 °C yielded the product as a white solid. Yield: 94.6% (9.51 g).

*2.2.2.2. MeOPEG-$N_3$.* MeOPEG-Cl (9.40 g, 1.87 mmol) was dissolved in 100 mL of anhydrous DMF and treated with $NaN_3$ (3.30 g, 50 mmol). The reaction mixture was stirred at 80 °C for 60 h, precipitated in 1 L of $Et_2O$ and filtered. The product was subsequently purified by dissolving it in 100 mL dichloromethane, washing with 200 mL of water, concentrating the organic layer to 50 mL under reduced pressure and its precipitation in 600 mL of 2-propanol. After filtration and drying in vacuum at 55 °C, the final product was obtained as white flakes. Yield: 70.9% (6.68 g). The IR of the product confirmed the absence of residual $NaN_3$, showing a single —$N_3$ peak

at 2117 $cm^{-1}$. $^1H$ NMR ($D_2O$) $\delta$ = 3.38 (s, 3H, —OC$H_3$), 3.45–3.95 (m, PEG chain protons).

#### 2.2.3. D40-18GP-18PEG

D40-18GP (0.150 g, 0.155 mmol alkynes) and MeOPEG-$N_3$ (1.32 g, 0.265 mmol) were dissolved in 16 mL of DMSO by warming at 50 °C. Subsequently TBTA (0.54 mL, 0.10 M in DMSO) and Na-Asc (0.17 mL, 0.28 M in water) were added to the solution, followed by bubbling with argon for 10 min. Finally, $Cu(MeCN)_4PF_6$ (23 mg, 0.062 mmol) was added to the reaction mixture, it was bubbled with argon for another 5 min and azide-alkyne cycloaddition (CuAAC) was performed under microwave irradiation (85 °C, 40 min). The reaction mixture was dialyzed against DMSO for 20 h, diluted with 250 mL of water and ultrafiltrated (MWCO 30,000). The product was obtained by freeze-drying as white solid (0.58 g). $^1H$ NMR (DMSO-$d_6$) $\delta$ = 2.90–3.90 (m, dextran glucosidic and PEG protons, overlapped with HDO), 4.40–5.20 (m, 4H, dextran hydroxyl + anomeric), 8.06 (s, 1H, triazole).

#### 2.2.4. D40-28GP-(5,10)Ada-(23,18)PEG

D40-28GP (0.160 g, 0.225 mmol alkyne) and Ada-$N_3$ (0.23–0.46 mL of a solution at 0.17 mol/L in DMSO) were dissolved in 17 mL of DMSO. TBTA (0.79 mL of a solution at 0.10 mol/L in DMSO) and Na-Asc (0.20 mL of a solution at 0.28 mol/L in water) were added, and the obtained solution was bubbled with argon for 10 min. Then, $Cu(MeCN)_4PF_6$ (50 mg, 0.132 mmol) was added, the reaction mixture was bubbled with argon for 5 min under sonication, followed by CuAAC, performed under microwave irradiation (70 °C, 20 min). Further, MeOPEG-$N_3$ (1.58–1.25 g, 0.32–0.25 mmol) was added to the reaction mixture and microwave irradiation was proceeded (85 °C, 40 min). The reaction mixture was dialyzed against DMSO for 20 h, diluted with 250 mL of water and ultrafiltrated (MWCO 30,000). The product was obtained by freeze-drying as white solid (0.69 g). $^1H$ NMR (DMSO-$d_6$) $\delta$ = 1.50 (s, 6H, Ada), 1.57–1.72 (m, 6H, Ada), 1.92 (s, 3H, Ada), 2.90–3.90 (m, dextran glucosidic and PEG protons, overlapped with HDO), 4.40–5.20 (m, 4H, dextran hydroxyl + anomeric), 8.06 (s, 1H, triazole-PEG), 8.10 (s, 1H, triazole-Ada).

### 2.3. Methods

#### 2.3.1. General methods

NMR measurements were performed in $D_2O$ or DMSO-$d_6$, unless other is indicated, on a Bruker Avance II Ultrashield Plus 400 MHz NMR spectrometer. $^1H$ NMR spectra were calibrated using the chemical shifts of the residual solvents signals according to the literature data (Fulmer et al., 2010). Fourier transform infrared spectroscopy (FT-IR) measurements were made on a Bruker Tensor 27 FT-IR spectrometer. Size exclusion chromatography coupled to multi-angle laser light scattering (SEC-MALLS) was performed in deionized water with 0.1 mol/L $LiNO_3$ (0.05% $NaN_3$) on TSK-gel type SW4000-3000 columns and detection by a Wyatt Dawn 8+ light scattering detector and a Wyatt Optilab Rex refractive index detector.

#### 2.3.2. Isothermal titration microcalorimetry

Isothermal titration microcalorimetry (ITC) measurements were performed using a MicroCal VPITC microcalorimeter. In each titration, injections of 10 μL of native βCD, pβCD or pβCDN+ solutions ($C_{\beta CD} = 5 \times 10^{-3}$ mol/L) were added from the computer controlled 295 μL microsyringe at an interval of 180 s into the cell ($V$ = 1.4569 mL) containing the investigated polymer solution ($5 \times 10^{-4}$ mol/L of Ada-groups) while stirring at 450 rpm. The temperature was fixed at 25 °C. The raw experimental data were obtained as the amount of heat produced per second following each injection of a host solution as a function of time. Integration of the heat flow peaks by the instrument software (after taking into account heat of dilution) provides the amount of heat produced per injection. The experimental data were fitted with a theoretical titration curve using the instrument software with a model assuming a 1:1 stoichiometry for the adamantyl/βCD complex. The enthalpy change, $|\Delta H|$, the association constant, $K_a$, and the overall stoichiometry were adjustable parameters.

#### 2.3.3. Surface plasmon resonance (SPR)

SPR measurements were carried out with a Spreeta SPR-EVM-BT from Texas Instruments. The light of an infrared light-emitting diode (LED; λ = 840 nm) reaches the sensor surface at a range of angles above the critical angle. A reflectivity-versus-angle spectrum is obtained, and an apparent refractive index (RI) is derived from it by the Spreeta software. The sensor surface is a gold layer (ca. 50 nm). In the case of adsorption on the golden surface the RI changes provide information on the adsorbed layer parameters. The sensor is integrated in a flow cell and the measurements were carried out at 23 °C using a continuous water flow (3 mL/h) which was delivered by a syringe pump (Kd Scientific), and a Rheodyne injection valve to switch to the sample solution.

The sensor surface was cleaned with a 4% $CrO_3$ solution in water and rinsed with MeOH before each experiment. After settling the sensor into the flow cell, an in situ cleaning was performed with one injection (0.1 mL) of a solution of 0.1 M NaOH and 1% Triton X-100 in water followed by 3 injections (0.1 mL) of 10% EtOH in water. The sensor was calibrated in pure water, assuming a RI value of 1.33300, and the RI variations after the different polymer injections were monitored as a function of time.

Two types of experiments were run. In the first type, three consecutive injections of 0.1 mL of pβCD in water or pβCDN+ in 0.5 M NaCl (both at 2 g/L) were carried out to saturate the gold surface of the sensor. This was followed by 3–4 consecutive injections (0.1 mL) of one of the PEG-containing dextrans in water with various DS by adamantyls (1 g/L). Then the RI variation due to the 2nd layer deposition was measured 20 min after the first injection.

In the second type, 1 mL of pβCDN+ solution at 0.2 g/L was injected to saturate the gold surface of the sensor; then an injection of 1 mL of the D40-28GP-10Ada-18PEG solution at various concentrations (0.01–0.1 g/L) was performed, and the kinetics of the adsorption were recorded and analyzed.

From the values of ΔRI the adsorbed amounts of the polymers may be estimated based on the following equation (Jung, Campbell, Chinowsky, Mar, & Yee, 1998):

$$\Delta RI = m(n_{pol} - n_s)\left[1 - \exp\left(\frac{-2d_{pol}}{l_d}\right)\right] \quad (1)$$

where $n_s$ and $n_{pol}$ are refractive indexes of the solvent and the polymer respectively, $d_{pol}$ is the thickness of deposited polymer layer and $l_d$ is the depth of penetration of the evanescent electromagnetic field (typically 25–50% of the probing light wavelength). In the present work it was roughly estimated as 37% (310.8 nm) (Jung et al., 1998; Wintgens & Amiel, 2005). We assumed $l_d$ to be constant upon each subsequent polymer adsorption, given the low density of highly hydrated layers and their thickness being much lower than 310.8 nm. The calibration coefficient $m$ of the sensor was estimated at 1.

Since $d_{pol} \ll l_d$, ΔRI is directly proportional to the layer thickness and Eq. (1) may be rewritten as:

$$\Delta RI = m(n_{pol} - n_s)\left(\frac{2d_{pol}}{l_d}\right) \quad (2)$$

The deposited polymer being highly swollen with the solvent leads $n_{pol} - n_s$ which means that:

$$n_{pol} - n_s = C_{surf}\left(\frac{dn}{dc}\right)_{pol} = \left(\frac{dn}{dc}\right)_{pol} \cdot \left(\frac{Q_{ads}}{d_{pol}}\right) \quad (3)$$

where $C_{surf}$ is the surface concentration and $Q_{ads}$ is the adsorbed amount of the polymer; $dn/dc$ is the RI increment of the polymer with respect to water. In this work it was assumed as 0.137 mL/g for both pβCD and pβCDN+ (Wintgens & Amiel, 2005). Combining Eqs. (2) and (3) one obtains:

$$Q_{ads} = \frac{\Delta RI \cdot l_d}{2m \cdot (dn/dc)_{pol}} \quad (4)$$

## 3. Results and discussion

### 3.1. Guest and host polymers

#### 3.1.1. D40-XGP-YAda-ZPEG preparation

Copper-catalyzed azide-alkyne cycloaddition (CuAAC) was chosen as an efficient tool to couple both adamantyl and MeOPEG moieties to the dextran backbone (Dedola, Nepogodiev, & Field, 2007; Hein, Liu, & Wang, 2008). Azide-substituted adamantane derivatives, azide-terminated MeOPEG and alkyne-substituted dextrans were chosen as building blocks for CuAAC.

Azide-substituted adamantane derivative (Ada-$N_3$, Fig. S1a in Supplementary data) was prepared according to the modified 2-step procedure used by Suzuki et al. (2010). It involves tosylation of 1-adamantaneethanol in pyridine followed by nucleophilic substitution with $NaN_3$ in DMSO. It should be noted that the obtained 1-adamantaneethyltosylate was not exposed to tedious column chromatography purification and after filtration on silica pad it contained some traces of native 1-adamantaneethanol. However it was not a problem due to its inability to react with $NaN_3$ in DMSO during the second step.

Azide-terminated MeOPEG (MeOPEG-$N_3$) was synthesized by a two-step procedure (Fig. S1b). The terminal hydroxyl of PEG was first converted to chloride with $SOCl_2$ according to a method previously described (Greenwald, Pendri, & Bolikal, 1995). The chloride was subsequently converted into azide by $S_N2$ substitution with an excess of $NaN_3$ in DMF. During the purification stage washing with water proved to be crucial for the full elimination of unreacted $NaN_3$.

Dextran of 40 kDa was modified with alkynes using the basic epoxide opening of glycidyl propargyl ether in water, according to the procedure described in literature (Nielsen, Wintgens, Amiel, Wimmer, & Larsen, 2010) (Fig. 1). The choice of the ether bond is justified by its hydrolytic stability and relatively long resulting spacer between the dextran backbone and grafted alkynes. The latter proved to be important for the preservation of good inclusion properties of subsequently grafted host–guest functions. The $^1H$ NMR spectrum of D40-28GP may be found in Supplementary data (Fig. S3).

In the next step D40-GP-Ada-PEG with various degrees of substitution were prepared by one-pot CuAAC (Fig. 1). Pure DMSO as a solvent and $Cu(MeCN)_4PF_6$/Na-Asc as a catalytic system were chosen due to poor solubility of Ada-$N_3$ in water. A Cu(I)-stabilizing polytriazole ligand TBTA was applied to prevent any undesirable acetylenic cross-couplings often encountered when dealing with alkyne polymeric scaffolds (Antoniuk, Volet, Wintgens, & Amiel, 2014; Nielsen et al., 2010; Siemsen, Livingston, & Diederich, 2000).

Typically in the first stage the aimed amount of Ada-$N_3$ was "clicked" quantitatively; then 1.6–1.8 equivalents of MeOPEG-$N_3$ were added to the reaction mixture to consume the residual alkynes. When performed under classical heating, due to the bulkiness of MeOPEG-$N_3$, the CuAAC required very long reaction times (3 days) for the second stage completion. Microwave-assisted heating was reported to significantly increase the reaction rates of CuAAC, especially when the reactants are bulky or polymeric units (Hoogenboom, Moore, & Schubert, 2006; Kappe & Van der Eycken, 2010). Indeed, when the same one-pot procedures were performed under microwave irradiation, the reaction times reduced dramatically. Full conversion of the residual alkynes by the reaction with MeOPEG-$N_3$ was typically achieved within 40 min at 85 °C.

By the MW-assisted heating approach, a set of D40-GP-Ada-PEG with various degrees of substitution by hydrophobic Ada (0–10 mol%) and by hydrophilic flexible MeOPEG chains (15–23 mol%) were obtained (Table 1). Whereas the $^1H$ NMR spectrum of D40-18GP-18PEG demonstrated a single triazole proton signal (Fig. S4), in the case of bifunctionalized

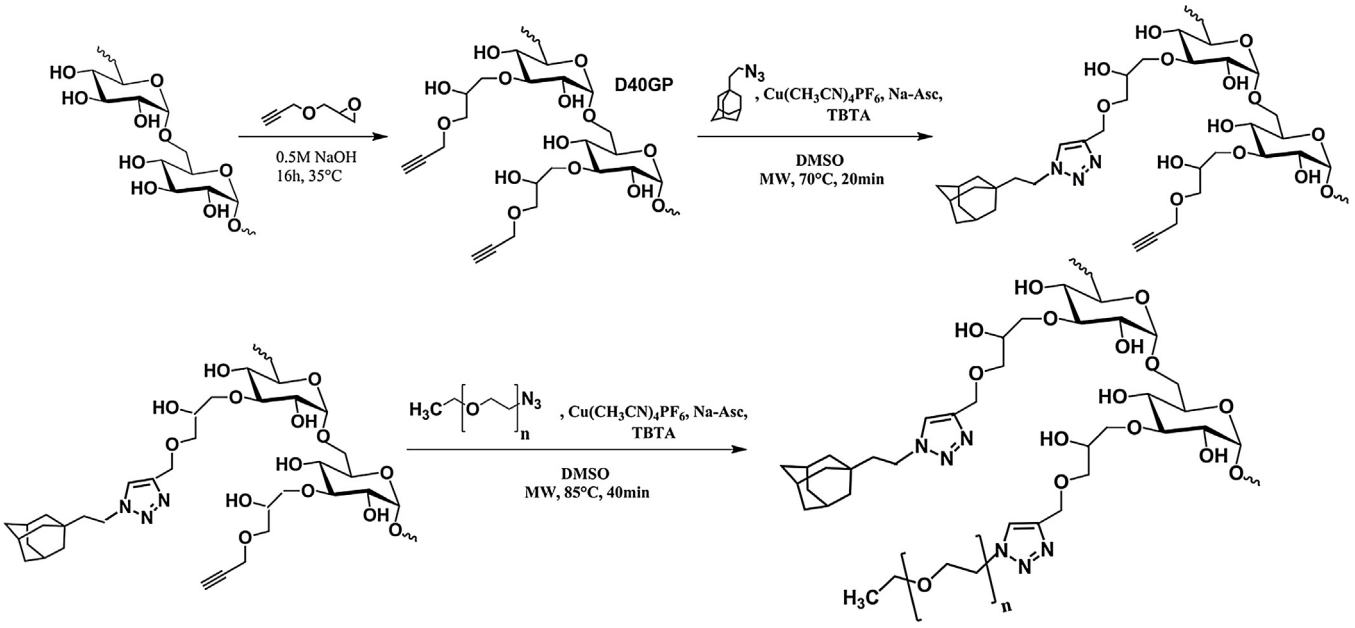


**Fig. 1.** Reaction scheme for the MW-assisted one-pot CuAAC synthesis of D40-GP-Ada-PEG.

**Table 1**
Characteristics of D40-XGP-YAda-ZPEG (guest) and pβCD (host) polymers.

| Guest polymers | GP, mol% | Ada, mol% | PEG, mol% |
|---|---|---|---|
| D40-18GP-18PEG | 18 | 0 | 18 |
| D40-28GP-5Ada-23PEG | 28 | 5 | 23 |
| D40-28GP-10Ada-18PEG | 28 | 10 | 18 |

| Host polymers | CD, wt% | $M_w$, kDa | N+/CD |
|---|---|---|---|
| pβCD | 67 | 208 | 0 |
| pβCDN+[a] | 65 | – | 1.62 |

[a] Prepared from pβCD.

D40-28GP-10Ada-18PEG one observes two distinct singlets at 8.06 and 8.10 ppm attributed to the PEG and Ada triazole protons respectively (Fig. S5).

### 3.1.2. pβCD host polymers

The "host" polymers, neutral epichlorhydrin-interconnected pβCD and positively charged pβCDN+, modified with quaternary ammonia, were prepared according to the previously reported procedure (Blomberg et al., 2004; Renard et al., 1997). These polymers have branched structure where βCD moieties may be thought of as balls interlinked by poly(2-hydroxypropyl)ether sequences of different lengths (Fig. S2a). Due to the seven-time excess of epichlorohydrin with respect to βCD, a part of it is consumed on the formation of polytails along with polybridges. The sample used in this work has a cyclodextrin weight ratio (g/g) of 65%, determined by $^1$H NMR, a molecular weight $M_w$ of 208 kDa, and a polydispersity index of 1.81, which were determined by size exclusion chromatography (SEC). To obtain positively charged host polymer, pβCD was modified with quaternary ammonia by reaction with 2,3-epoxypropyltrimethylammonium (Fig. S2b). The characteristics of all the host and guest polymers are reported in Table 1.

## 3.2. ITC studies

The ability of D40-GP-Ada-PEG to form inclusion complexes with βCD and βCD-polymers was examined by isothermal titration microcalorimetry (ITC). The interactions of the polymers with monomeric βCD are highly exothermic (Table 2) as expected, given the perfect matching in size between grafted Ada and βCD-cavities leading to strong van der Waals interactions between them. The fits of the titration curves (Fig. 2a) were done applying a simple 1:1 interaction model, where one assumes that each of the adamantyl groups grafted on one chain (12–25 per chain) acts independently from the others. The different thermodynamic parameters derived from these experiments are given in Table 2. The association constants are as high as $4.0–6.0 \times 10^4$ L/mol, which is superior to previously described dextrans modified with Ada-groups via simple esterification by 1-adamantanecarbonyl chloride (Wintgens et al., 2011). It might be explained by the presence of relatively long and hydrophilic spacer in D40-GP-Ada-PEG, the latter making adamantyl groups more loosely attached and available for complexation. As in the reference (Wintgens et al., 2011), a slight decrease of $K_a$ is observed while increasing the substitution degree by Ada-groups from 5 to 10 mol%, which could be attributed to a gradual loss of their accessibility due to steric effects.

In the next step we applied ITC to study the interpolymer interactions. The concentration of adamantyl groups in the solutions of D40-GP-Ada-PEGs was fixed at $5 \times 10^{-4}$ mol/L. The solution of D40-18GP-18PEG, bearing no adamantyl groups, was used at the mass concentration equal to that of D40-28GP-10Ada-18PEG with $C_{Ada} = 5 \times 10^{-4}$ mol/L. The enthalpograms, shown in Fig. 2b and c are plotted as a function of the βCD/Ada molar ratio. Except for the case of D40-18GP-18PEG (free of adamantyl groups) where no interaction could be detected (black circles in Fig. 2b and c), the guest polymers display highly exothermic interactions with both host polymers (pβCD and pβCDN+).

Likewise for monomeric βCD, the fits are done assuming a simple 1:1 interaction model. The imperfect matching between the experimental points and the fitting curves could be attributed to slight correlations between the interaction sites within a same chain. Nevertheless the fits allowed us to estimate thermodynamic parameters of the interactions, reported in Table 2. The interactions strength is strongly dependent on the adamantyl content of the guest polymers. In the case of titration by pβCD, $K_a$ becomes almost one order of magnitude higher in favor of D40-28GP-10Ada-18PEG – more substituted by adamantyl groups and less by PEG chains. Such behavior might be ascribed to interplay between the cooperativity effects of neighboring adamantyl groups and steric hindrance arising from PEG grafts. One can suppose that D40-28GP-5Ada-23PEG is less likely to approach and form stable complexes with pβCD due to a lower number of linking points (5 mol% Ada) and higher density of bulky PEG grafts. The evolution of the $T\Delta S$ values is in agreement with this assumption: significantly negative $T\Delta S$ values at 5 mol% Ada, which could correspond to anti-cooperative binding, switch to positive $T\Delta S$ values at 10 mol% Ada, giving an indication of more cooperative binding.

The same tendency was observed in the case of titration by charged pβCDN+. Interestingly, the binding constants for the polymer bearing 5 mol% of adamantyl groups are of the same order for pβCD and pβCDN+; on the other hand for the 10 mol% polymer, $K_a$ is pronouncedly higher when titrated by pβCDN+ (Table 2).

Given the results above, in the next step we were interested in evaluation and comparison of the binding properties of (PEG, adamantyl)-grafted dextrans on the surface by SPR.

## 3.3. SPR adsorption studies

To perform SPR binding experiments, βCD-polymers were deposited as a 1st layer on the golden surface of the sensor. When either pβCD or pβCDN+ solution is flowed over the sensor surface, the RI increases due to the physical adsorption of CD-polymers, which should be driven by non-specific and electrostatic interactions between the polymers and the gold surface. Typically 3 injections of 2 g/L solutions were enough to reach the plateau in RI, indicating the surface saturation, as shown in the first part of the sensorgrams for neutral pβCD (Fig. 3). It should be noted that in Fig. 4 the transient increase in RI during the host polymer injections

**Table 2**
Thermodynamic parameters of interaction of the D40-GP-Ada-PEG polymers with monomeric βCD and βCD-polymers at 25 °C.

| Titrant | Ada, mol% | $K_a \times 10^{-3}$, L/mol | $\Delta H$, kJ/mol | $T\Delta S$, kJ/mol | $\Delta G$, kJ/mol |
|---|---|---|---|---|---|
| βCD | 5 | 60.7 | −44.4 | −16.9 | −27.4 |
| | 10 | 40.3 | −41.6 | −15.2 | −26.3 |
| pβCD | 5 | 3.34 | −40.0 | −19.8 | −20.2 |
| | 10 | 21.9 | −21.7 | 3.0 | −24.8 |
| pβCDN+ | 5 | 3.02 | −35.6 | −15.7 | −19.8 |
| | 10 | 35.4 | −18.1 | 7.8 | −26.0 |

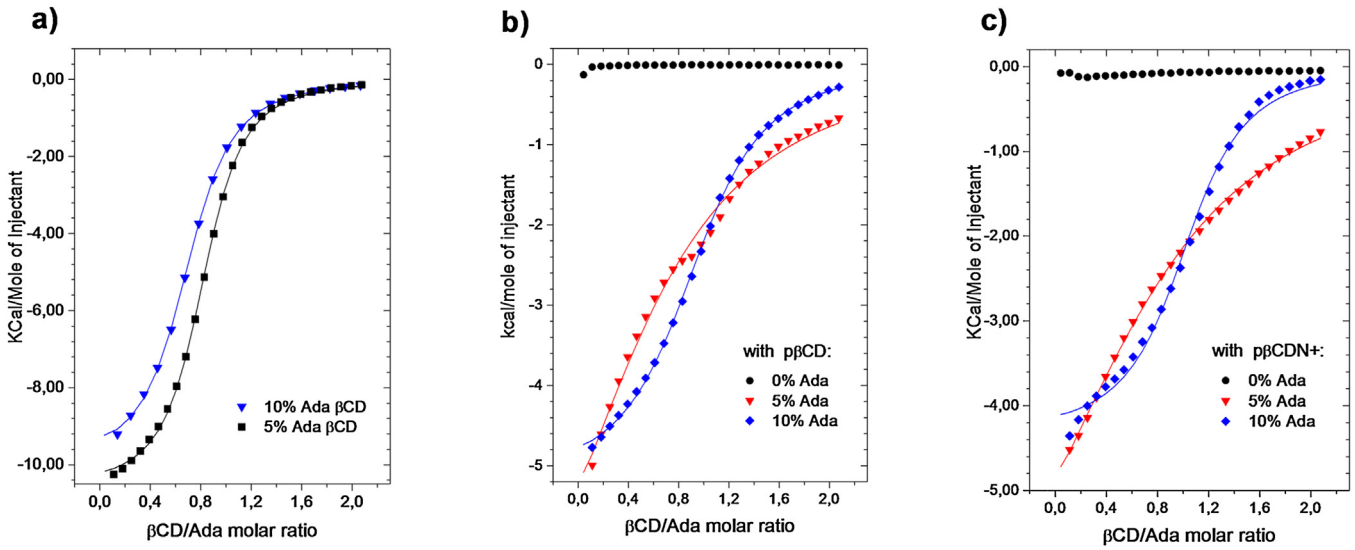


**Fig. 2.** Enthalpograms of the interaction of D40-GP-Ada-PEG polymers with monomeric βCD (a), pβCD (b), and pβCDN+ (c). The solid lines represent the fits of the data by One Set of Sites model (Origin 7.0 ITC custom version).

is due to pβCDN+ being dissolved in 0.5 M NaCl solution. The resulting 1st layer obtained after equilibration for 20 min gives a quite stable ΔRI in both cases ($8.5 \times 10^{-4} \pm 0.8$ and $12.1 \times 10^{-4} \pm 0.7$ for pβCDN+ and pβCD respectively).

The adsorbed amounts of the polymers may be estimated based on Eq. (4). Calculations showed that the adsorbed amount is roughly 1.4 times higher for the neutral pβCD – 1.37 mg/m$^2$ – than for the charged pβCDN+ – 0.97 mg/m$^2$. The poorer adsorption characteristics of pβCDN+ might be related to strong hydration and spatial extension of the charged molecules, which prevents them from forming a strong linkage to the surface. In support of this it should be noted that when pβCDN+ solution in pure $H_2O$ is used, i.e. electrostatic repulsions are not screened at all, only negligible amounts are adsorbed.

The next step was to investigate the adsorption of the D40-GP-Ada-PEG polymers on the preformed pβCD-layer as a function of their DS by adamantyl groups. The results obtained in the case of neutral pβCD as the 1st layer are shown in Fig. 3. One can observe

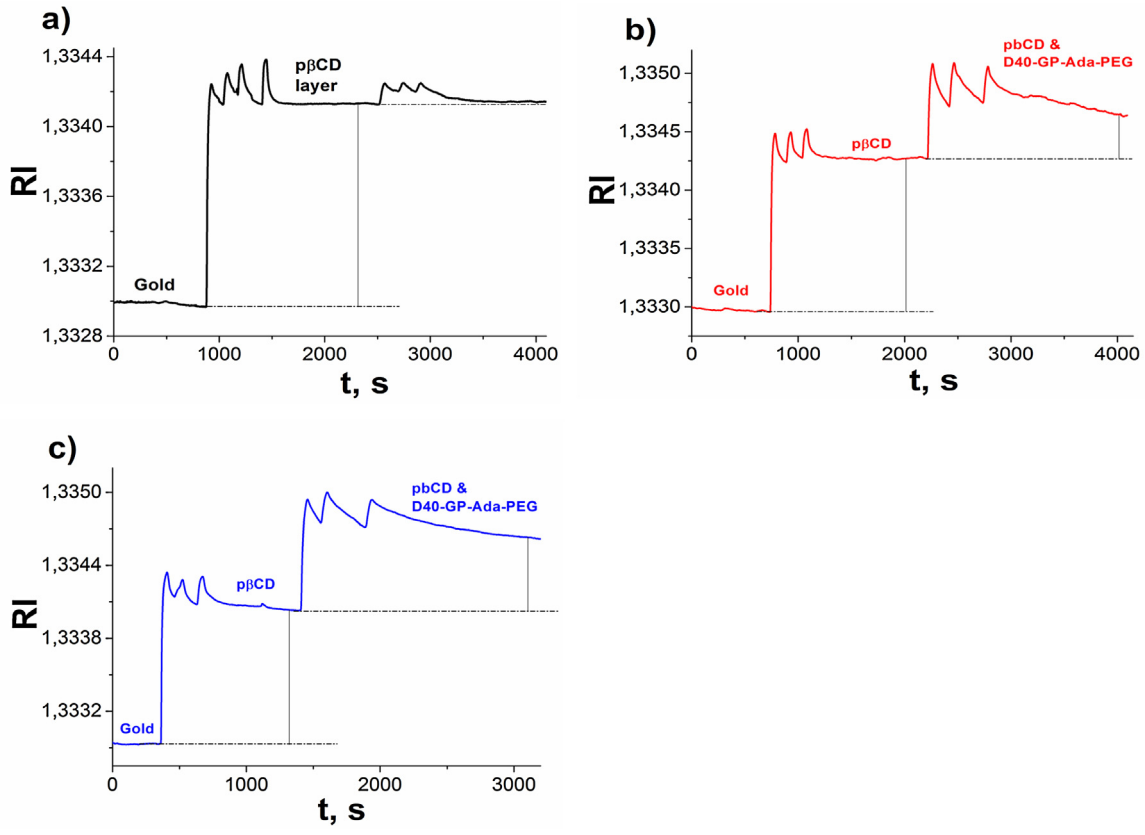


**Fig. 3.** Adsorption of D40-GP-Ada-PEG on neutral pβCD layer. DS(Ada): 0 (a), 5 (b), and 10 (c) mol%.

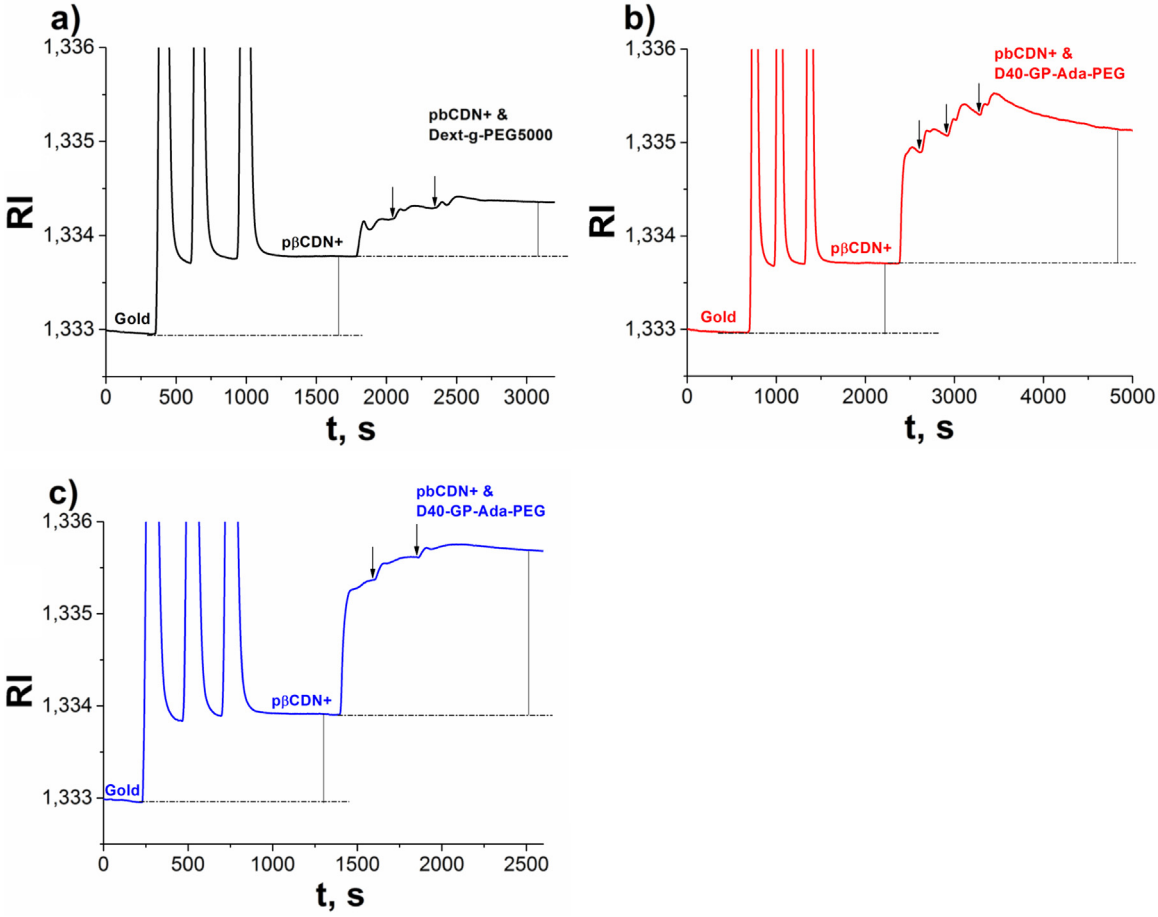


**Fig. 4.** Adsorption of D40-GP-Ada-PEG on pβCDN+ with 1.6 $N^+$ per CD. DS(Ada): 0 (a), 5 (b), and 10 (c) mol%. The consecutive injections are indicated by arrows.

that for the polymer bearing no adamantyl groups there is no deposition of the 2nd layer with ΔRI going back to zero after the flow of water for ca. 15 min (Fig. 3a). This indicates that non-specific adsorption onto the gold surface has been prevented by the first layer of neutral pβCD and that there is no detectable interaction between the pβCD layer and D40-18GP-18PEG. This finding correlates with the solution ITC studies results (see Section 3.2).

For the polymer bearing 5 mol% of adamantyl groups, clear formation of the 2nd layer was observed after the 3 successive injections. However a gradual desorption takes place as water is flowed for ~30 min, indicating that the deposited polymer is rather loosely attached (Fig. 3b). When the DS(Ada) is raised to 10 mol% the deposited D40-GP28-Ada10-PEG18 layer becomes more firmly anchored and the ΔRI after equilibration in water is increased by 30% (Fig. 3c). The content of PEG in all investigated polymers was at ca. 80–85 wt%. Therefore we assumed them to have a *dn*/*dc* equal to that of pure MeOPEG-OH (0.135 mL/g) in order to calculate the adsorbed amounts (after 30 min of equilibration in water).

The obtained results (Fig. 5) show that the adsorption of the D40-GP-Ada-PEG polymers onto non-charged pβCD is predominantly driven by host–guest interactions. Moreover, higher adamantyl substitution degree appears to be responsible for the formation of thicker and more stable 2nd layer.

The situation is quite different when pβCDN+ is used as the 1st layer (Fig. 4). Even D40-18GP-18PEG with no Ada functions leads to formation of the 2nd layer with an adsorbed amount of 0.63 mg/$m^2$ (Fig. 5). It also shows no significant decrease in ΔRI during the equilibration period (20 min) in water, indicating strong binding between the layers (Fig. 4a). For D40-GP28-Ada5-PEG23 the adsorbed amount is ca. 3 times higher, but at the initial stage of equilibration a part of it is washed out with the flow of water (Fig. 4b). Finally, for the D40-GP28-Ada10-PEG18 the adsorbed amount is further increased and the layer gains in stability (Fig. 4c). Interestingly, the adsorption pattern on pβCDN+ is changed as well. No or little decrease in refractive index is observed straight after each consecutive injection. One can assume that due to the higher strength of interpolymer interaction with pβCDN+, there are less of loosely anchored D40-*X*GP-*Y*Ada-*Z*PEG molecules which are washed out after the adsorption.

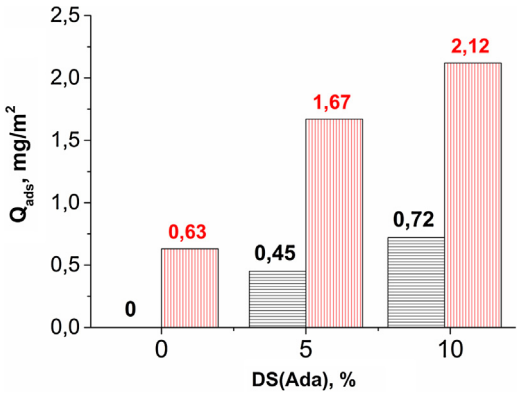


**Fig. 5.** The adsorbed amounts of D40-GP-Ada-PEG with various DS(Ada): on pβCD (black bars, horizontal pattern); on pβCDN+ (red bars, vertical pattern). (For interpretation of the references to color in this figure legend, the reader is referred to the web version of this article.)

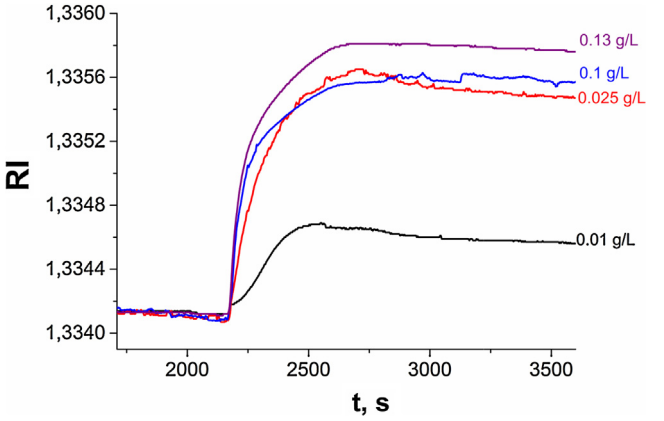


**Fig. 6.** The evolution of RI versus time for various D40-28GP-10Ada-18PEG concentrations flowed over a pβCDN+ layer.

Contrarily to the ITC study where no interaction could be detected between D40-GP-PEG and pβCDN+ in solution (Section 3.2), the same polymer (D40-GP-PEG) leads to a non-negligible interaction onto the gold/pβCDN+ surface. There is probably a contribution of the gold surface which is not as fully saturated with pβCDN+ as in the case of pβCD. However this cannot fully explain the quite large adsorbed amount. As polysaccharides and polysaccharide-based nanoassemblies are typically characterized by slightly negative values of zeta potential (Wintgens et al., 2011), non-specific electrostatic interactions could also be at the origin of the enhanced interpolymer interaction. Given that, the adsorption behavior of D40-GP-Ada-PEG on the positively charged pβCDN+-layer might be related to interplay between the host–guest and reinforced non-specific interactions in the system. Accordingly, the adsorbed amounts of D40-GP-Ada-PEG on pβCDN+ are roughly 3 times higher compared to the neutral pβCD (Fig. 5).

### 3.4. Reaction kinetics by SPR

The kinetics parameters of interaction of D40-28GP-10Ada-18PEG with positively charged pβCDN+ were evaluated given that the latter has demonstrated the most interesting SPR adsorption profile (Fig. 5). First, the gold surface was saturated with pβCDN+, and then D40-28GP-10Ada-18PEG solutions at various concentrations (0.01–0.20 g/L) were passed over the pβCDN+ layer. The results are represented in Fig. 6. At low concentrations (e.g. 0.01 g/L), the RI increases quasi-linearly with time, indicating that every polymer molecule reaching the surface should be adsorbed in this case. The adsorbed amount corresponding to the plateau (0.59 mg/m$^2$) is less than 30% of the saturation amount, obtained from the SPR adsorption experiment (see Section 3.3). The sensorgram recorded at 0.025 g/L changes its character drastically (Fig. 6). One observes a steep initial growth with 1.65 mg/m$^2$ of the deposited polymer at the plateau, which is already 78% of the saturation value. When increasing the concentration up to 0.1 g/L and higher, the initial exponential growth becomes even steeper and the amount of adsorbed polymer at the plateau gradually approaches the saturation level from the experiment with multiple injections of the 1 g/L solution (Fig. 5). The above is an indication of strong affinity between the polymers. Indeed, at such low concentrations as 0.025 g/L one already observes a fast exponential saturation of the surface sites of pβCDN+.

Since the obtained sensorgrams contain continuous real-time data, they can be used for evaluation of the kinetics of the interpolymer interaction. For the first part of the sensorgram (until $RI_{max}$ is reached) the interaction might be schematically written as:

$$[R-Ada]^{sol.} + [R-CD]^{surf.} \rightleftarrows [Complex]^{surf.} \quad (5)$$

In this case the variation of RI versus time, due to complexation, is expressed by the following equation (Oshannessy, Brighamburke, Soneson, Hensley, & Brooks, 1993):

$$\frac{dRI}{dt} = k_a C_{Ada}(RI_{max} - RI) + k_d \quad (6)$$

where $C_{Ada}$ is the concentration of adamantyl groups in the injected solution. The $k_a$ and $k_d$ constants are obtained by fitting the experimental curves for the polymer concentrations ≥0.025 g/L to the integrated form of the dependence of RI versus time:

$$RI(t) = \frac{C_{Ada}k_a[R]_{max} - RI(0)[1 - \exp(-C_{Ada}k_a + k_d t)]}{C_{Ada}k_a + k_d} \quad (7)$$

in which RI(0) is the refractive index in the moment of injection ($t = 0$).

The average values of $k_a$ and $k_d$ obtained from the sensorgrams recorded at polymer concentrations varying in the range 0.08–0.20 g/L are of $7.0 \times 10^2$ mol$^{-1}$ s$^{-1}$ and $1.1 \times 10^{-3}$ s$^{-1}$ (more details in Table S1); examples of the fits may be found in the Supporting data (Fig. S6). From this one can calculate the association constants $K_a$ using the following equation:

$$K_a = \frac{k_a}{k_d} \quad (8)$$

The estimated average $K_a = 6.4 \times 10^5$ L/mol is more than one order of magnitude higher than the one determined for the interaction in solution ($K_a = 3.5 \times 10^4$ L/mol, Table 2); it is also roughly 3 times higher than the $K_a$ between native βCD and monomeric adamantane derivatives (Nielsen et al., 2010). This large $K_a$ increase compared to the one determined in solution has been reported previously for polymeric guests and is attributed to increased cooperative interactions, the host moieties being constrained in close proximity on the surface (Wintgens & Amiel, 2005). Moreover, $K_a$ is one order of magnitude higher than the previously reported $K_a$ between pβCD and adamantyl modified PNIPAMs (PNIPAM-Ada) on gold surface (Wintgens & Amiel, 2005), thus indicating an excellent affinity of D40-GP-Ada-PEG to pβCDN+. More specifically, association rate constants $k_a$ (700 mol$^{-1}$ s$^{-1}$) are around 3 times higher than the ones determined for PNIPAM-Ada/pβCD (Wintgens & Amiel, 2005) or for adamantyl carboxylic acid/βCD systems (Busse, DePaoli, Wenz, & Mittler, 2001). At the same time the dissociation rate constants $k_d$ ($1.1 \times 10^{-3}$ s$^{-1}$) are more than one order of magnitude lower than those for monomeric host–guest interactions (adamantyl carboxylic acid/βCD) and 3 times lower than for PNIPAM-Ada/pβCD multivalent interactions case. The larger $k_a$ and the lower $k_d$ than expected can be related to the previously mentioned additional interactions arising between D40-GP-Ada-PEG and pβCDN+ at interfaces, leading to larger adsorption and slower desorption rates.

## 4. Conclusion

A series of new (PEG, Ada)-grafted dextrans have been prepared using copper(I)-catalyzed azide-alkyne cycloaddition. Due to the presence of longer and more flexible spacer between the adamantyl groups and the dextran backbone, the polymers show significant improvement of their surface binding properties comparing to the previously described hydrophobically modified PNIPAms. Moreover, their ability to form inclusion complexes with monomeric βCD, neutral poly-βCD and cationic poly-βCDN+, both in solution and on surface, proves to be strongly dependent on the degree of substitution by Ada-functions, giving indications of cooperativity

effects between them. Given the above, (PEG, Ada)-grafted dextrans should be auspicious candidates for biomedical applications where fast and reversible PEGylation is required.

## Acknowledgement

This work has been supported by the European Commission for Research in the Framework of NanoS3 Marie Curie Initial Training Network (Grant agreement no.: 290251).

## Appendix A. Supplementary data

Supplementary data associated with this article can be found, in the online version, at doi:10.1016/j.carbpol.2015.07.027

## References

Antoniuk, I., Volet, G., Wintgens, V., & Amiel, C. (2014). Synthesis of a new dextran-PEG-b-cyclodextrin host polymer using "Click" chemistry. *Journal of Inclusion Phenomena and Macrocyclic Chemistry*, *80*, 93–100.

Blomberg, E., Kumpulainen, A., David, C., & Amiel, C. (2004). Polymer bilayer formation due to specific interactions between beta-cyclodextrin and adamantane: A surface force study. *Langmuir*, *20*(24), 10449–10454.

Brewster, M. E., & Loftsson, T. (2007). Cyclodextrins as pharmaccutical solubilizers. *Advanced Drug Delivery Reviews*, *59*(7), 645–666.

Busse, S., DePaoli, M., Wenz, G., & Mittler, S. (2001). An integrated optical Mach–Zehnder interferometer functionalized by beta-cyclodextrin to monitor binding reactions. *Sensors and Actuators B: Chemical*, *80*(2), 116–124.

Chan, T. R., Hilgraf, R., Sharpless, K. B., & Fokin, V. V. (2004). Polytriazoles as copper(I)-stabilizing ligands in catalysis. *Organic Letters*, *6*(17), 2853–2855.

David, C., Millot, M. C., Sebille, B., & Levy, Y. (2003). The reversible binding of hydrophobically end-capped poly(ethylene glycol)s to poly-beta-cyclodextrin-coated gold surfaces: A surface plasmon resonance investigation. *Sensors and Actuators B: Chemical*, *90*(1–3), 286–295.

Dedola, S., Nepogodiev, S. A., & Field, R. A. (2007). Recent applications of the Cu-I-catalysed Huisgen azide-alkyne 1,3-dipolar cycloaddition reaction in carbohydrate chemistry. *Organic & Biomolecular Chemistry*, *5*(7), 1006–1017.

El Fagui, A., & Amiel, C. (2012). PLA nanoparticles coated with a beta-cyclodextrin polymer shell: Preparation, characterization and release kinetics of a hydrophobic compound. *International Journal of Pharmaceutics*, *436*(1–2), 644–651.

Fulmer, G. R., Miller, A. J. M., Sherden, N. H., Gottlieb, H. E., Nudelman, A., Stoltz, B. M., et al. (2010). NMR chemical shifts of trace impurities: Common laboratory solvents, organics, and gases in deuterated solvents relevant to the organometallic chemist. *Organometallics*, *29*(9), 2176–2179.

Gaucher, G., Dufresne, M. H., Sant, V. P., Maysinger, D., & Leroux, J. C. (2005). Block copolymer micelles: Preparation, characterization and application in drug delivery. *Journal of Controlled Release*, *109*(1–3), 169–188.

Greenwald, R. B., Pendri, A., & Bolikal, D. (1995). Highly water soluble taxol derivatives: 7-Polyethylene glycol carbamates and carbonates. *Journal of Organic Chemistry*, *60*(2), 331–336.

Hedges, A. R. (1998). Industrial applications of cyclodextrins. *Chemical Reviews*, *98*(5), 2035–2044.

Hein, C. D., Liu, X. M., & Wang, D. (2008). Click chemistry, a powerful tool for pharmaceutical sciences. *Pharmaceutical Research*, *25*(10), 2216–2230.

Hoogenboom, R., Moore, B. C., & Schubert, U. S. (2006). Synthesis of star-shaped poly(epsilon-caprolactone) via 'click' chemistry and 'supramolecular click' chemistry. *Chemical Communications*, (38), 4010–4012.

Immordino, M. L., Dosio, F., & Cattel, L. (2006). Stealth liposomes: Review of the basic science, rationale, and clinical applications, existing and potential. *International Journal of Nanomedicine*, *1*(3), 297–315.

Jokerst, J. V., Lobovkina, T., Zare, R. N., & Gambhir, S. S. (2011). Nanoparticle PEGylation for imaging and therapy. *Nanomedicine*, *6*(4), 715–728.

Jung, L. S., Campbell, C. T., Chinowsky, T. M., Mar, M. N., & Yee, S. S. (1998). Quantitative interpretation of the response of surface plasmon resonance sensors to adsorbed films. *Langmuir*, *14*(19), 5636–5648.

Kappe, C. O., & Van der Eycken, E. (2010). Click chemistry under non-classical reaction conditions. *Chemical Society Reviews*, *39*(4), 1280–1290.

Li, S. D., & Huang, L. (2008). Pharmacokinetics and biodistribution of nanoparticles. *Molecular Pharmaceutics*, *5*(4), 496–504.

Loftsson, T., & Brewster, M. E. (1996). Pharmaceutical applications of cyclodextrins. 1. Drug solubilization and stabilization. *Journal of Pharmaceutical Sciences*, *85*(10), 1017–1025.

Loira-Pastoriza, C., Todoroff, J., & Vanbever, R. (2014). Delivery strategies for sustained drug release in the lungs. *Advanced Drug Delivery Reviews*, *75*, 81–91.

Nielsen, T. T., Wintgens, V., Amiel, C., Wimmer, R., & Larsen, K. L. (2010). Facile synthesis of beta-cyclodextrin-dextran polymers by "Click" chemistry. *Biomacromolecules*, *11*(7), 1710–1715.

Oshannessy, D. J., Brighamburke, M., Soneson, K. K., Hensley, P., & Brooks, I. (1993). Determination of rate and equilibrium binding constants for macromolecular interactions using surface plasmon resonance: Use of nonlinear least squares analysis methods. *Analytical Biochemistry*, *212*(2), 457–468.

Pun, S. H., & Davis, M. E. (2002). Development of a nonviral gene delivery vehicle for systemic application. *Bioconjugate Chemistry*, *13*(3), 630–639.

Quaglia, F., De Rosa, G., Granata, E., Ungaro, F., Fattal, E., & La Rotonda, M. I. (2003). Feeding liquid, non-ionic surfactant and cyclodextrin affect the properties of insulin-loaded poly(lactide-co-glycolide) microspheres prepared by spray-drying. *Journal of Controlled Release*, *86*(2–3), 267–278.

Ren, S. D., Chen, D. Y., & Jiang, M. (2009). Noncovalently connected micelles based on a beta-cyclodextrin-containing polymer and adamantane end-capped poly(epsilon-caprolactone) via host–guest interactions. *Journal of Polymer Science Part A: Polymer Chemistry*, *47*(17), 4267–4278.

Renard, E., Deratani, A., Volet, G., & Sebille, B. (1997). Preparation and characterization of water soluble high molecular weight beta-cyclodextrin-epichlorohydrin polymers. *European Polymer Journal*, *33*(1), 49–57.

Roberts, M. J., Bentley, M. D., & Harris, J. M. (2002). Chemistry for peptide and protein PEGylation. *Advanced Drug Delivery Reviews*, *54*(4), 459–476.

Siemsen, P., Livingston, R. C., & Diederich, F. (2000). Acetylenic coupling: A powerful tool in molecular construction. *Angewandte Chemie International Edition*, *39*(15), 2633–2657.

Suzuki, T., Ota, Y., Kasuya, Y., Mutsuga, M., Kawamura, Y., Tsumoto, H., et al. (2010). An unexpected example of protein-templated click chemistry. *Angewandte Chemie International Edition*, *49*(38), 6817–6820.

van de Manakker, F., Vermonden, T., van Nostrum, C. F., & Hennink, W. E. (2009). Cyclodextrin-based polymeric materials: Synthesis, properties, and pharmaceutical/biomedical applications. *Biomacromolecules*, *10*(12), 3157–3175.

Versluis, F., Voskuhl, J., Vos, J., Friedrich, H., Ravoo, B. J., Bomans, P. H. H., et al. (2014). Coiled coil driven membrane fusion between cyclodextrin vesicles and liposomes. *Soft Matter*, *10*(48), 9746–9751.

Volet, G., & Amiel, C. (2012). Polyoxazoline adsorption on silica nanoparticles mediated by host–guest interactions. *Colloids and Surfaces B: Biointerfaces*, *91*, 269–273.

Vonarbourg, A., Passirani, C., Saulnier, P., & Benoit, J. P. (2006). Parameters influencing the stealthiness of colloidal drug delivery systems. *Biomaterials*, *27*(24), 4356–4373.

Wintgens, V., & Amiel, C. (2005). Surface plasmon resonance study of the interaction of a beta-cyclodextrin polymer and hydrophobically modified poly(N-isopropylacrylamide). *Langmuir*, *21*(24), 11455–11461.

Wintgens, V., Layre, A. M., Hourdet, D., & Amiel, C. (2012). Cyclodextrin polymer nanoassemblies: Strategies for stability improvement. *Biomacromolecules*, *13*(2), 528–534.

Wintgens, V., Nielsen, T. T., Larsen, K. L., & Amiel, C. (2011). Size-controlled nanoassemblies based on cyclodextrin-modified dextrans. *Macromolecular Bioscience*, *11*(9), 1254–1263.

Wu, L. F., & Brazel, C. S. (2008). Modifying the release of proxyphylline from PVA hydrogels using surface crosslinking. *International Journal of Pharmaceutics*, *349*(1–2), 144–151.

Yoncheva, K., Lizarraga, E., & Irache, J. M. (2005). Pegylated nanoparticles based on poly(methyl vinyl ether-co-maleic anhydride): Preparation and evaluation of their bioadhesive properties. *European Journal of Pharmaceutical Sciences*, *24*(5), 411–419.